

Modelling of Electric Field Distribution in A Non-thermal Plasma Reactor Using COMSOL Multiphysics

M. Mortazavi¹, L. Amato¹, N. Manivannan², Maysam Abbod¹, W. Balachandran¹

1. Electronic and Electrical Engineering Department, Brunel University London, Uxbridge, London, United Kingdom

2. School of Design, Brunel University London, Uxbridge, London, United Kingdom

Abstract

The importance of the electric field and charged particles dynamics in various applications including plasma reactors has been recognized more than ever. Furthermore, the role of the multiphysics modelling and simulation in the process of investigation, design and product prototyping is also becoming more popular due to increased speed of computers and advanced software techniques. In this work, electric field distribution in a non-thermal plasma (NTP) reactor has been studied using COMSOL multiphysics for the application of NO_x reduction in the emission control. NTP was created in dielectric barrier discharge (DBD) cylindrical reactor with high voltage- ground electrodes. This study investigates the electric field distribution in non-thermal plasma under different reactor configurations. We investigated electric field distribution with and without applying space charge density; reactor design with multi ground electrodes, reactor design with a 1.2 m ground electrode and variable HV electrode dimensions. This study has provided an overall insight on the electric field distribution in non-thermal plasma and can be used as a guide for the electric field behaviour within a nitrogen gas non-thermal plasma.

Keywords: COMSOL modelling, NON-Thermal Plasma, Electric field in Plasma, DBD Plasma

1. Introduction

The state-of-the-art technology is moving towards more complex and multidisciplinary processes and systems. There is a growing interest in using multi-physics simulations to have a better understanding of the underpinning science of the processes as well as providing cost-effective solutions leading to practically achievable systems and products. The importance of the electric field and charged particles dynamics in various applications including but not limited to batteries, plasma reactors, healthcare, manufacturing, food industries and climate studies has been recognized more than ever and it has highlighted the need for an in-depth understanding of the electrodynamics in such processes using computer modelling and simulations. In this work, electric field distribution in a non-thermal plasma reactor has been studied using COMSOL Multiphysics.

Plasma science has been of specific interest during last three decades and its applications have been expanded into different industrial fields. Plasma can be generated by applying sufficient energy such as electric field energy, thermal energy, radiations, to a neutral gas, and is characterized by the existence of a mixture of free electrons, excited species, radicals, and ions.

Non-thermal plasma (NTP) process occurs under extremely non-equilibrium conditions for all species. It distinguishes from the thermal plasma as the species are in their excited state, but their kinetic energy is much lower than the electrons. In fact, even if the electron temperature is high (1-10 eV mean electron energy) the gas temperature can be maintained low [1]. The high concentration of species in their excited state allows the chemical reactions that require high activation energy to occur. The reduction in the activation energy barrier makes NTP an alternative technology to catalysts process to produce species that are not favoured at the room temperature.

Plasma can be created from most gaseous mixtures among them are oxygen, nitrogen, and dry air. Collisions between energetic electrons and gas molecules generate a blend of reactive species. The basic fact of NTP is that electron temperature (T_e) is much lower than gas temperature (T_g), where $T_e \gg T_g$ [2].

NTP is generated by high intensity electric field excited discharges in different approaches including dielectric barrier discharge (DBD), corona discharges (CD), local Townsend discharge (LTD), constricted glows (CG) and electron avalanches (EA).

DBD plasma is one of the prominent technologies in generating NTP under the atmospheric pressure and ambient temperature [3]. Atmospheric pressure DBD has been used for different applications such as sterilization biological decontamination, ozone production, surface modification, decontamination of environmental pollutant and water treatment [4, 5]. DBD discharge often forms with streamer breakdown procedure in a non-uniform electric field. The streamers are the results of an avalanche of electrons produced by high intensity electric field. The collisions of the electrons with neutral gas molecules generate a cloud of positive and negative charges in the gas phase that represents the plasma. When the breakdown field is achieved, the NTP is produced while attachment of electrons to other heavy particles and recombining of products reduces the NTP conductivity and as a result, it is terminated. If the electric field strength is lower than the breakdown field strength, this discharge and consequently NTP is affected. The effective parameters in generation and maintaining the NTP in the reactor, in addition to the chemistry of the plasma, are dielectric properties and thickness, geometry of the electrodes and the size of the discharge gap (distance between electrodes).

A better understanding of the underpinning physics and precise analysis of the DBD reactor can increase the efficiency of the NTP process and improve the outcome of the intended activity. DBD can be designed in different configurations based on the application. The multiphysics simulation would facilitate the reactor design optimization considering electrodes' size and shape, dielectric materials, applied voltages and frequency.

In this work, electric field distribution of a designed reactor is investigated under different scenarios. Firstly, the electric field distribution within the reactor was investigated when a potential of 20kV was applied to the active electrode with and without the presence of free space charge. Second, scenario is to assess the effect of ground electrode design on the electric field distribution and thirdly, the effect of the HV electrode diameter on the electric field distribution was investigated. In the second and third cases space charge density was not included.

2. Theory / Experimental Set-up

Complex nature of the plasma chemistry consisting of various reactions and different products and their wide range timescale characteristics, are a challenge when it comes to modelling and simulation and it creates computational difficulties and costly simulations.

The plasma chemistry including excitation, de-excitation, ionization, and recombination processes are in the range of micro-seconds time scale and needs high volume of computational tasks. Therefore, most plasma models available in literature are 1D to consume less computing time and cost.

However, having the benefit of electrostatics interface in the AC/DC module in COMSOL and eliminating the chemical reactions calculations, this investigation was done in 3D. The simulation is a stationary study when 20 kV is applied on the HV electrode surface

The model considered a cylindrical Dielectric Barrier Discharge plasma reactor with an axial high voltage (HV) electrode surrounded by a cylindrical glass tube as dielectric with a ground electrode on the outer circumference of the dielectric. Non-thermal plasma is generated using nitrogen gas that occupies the space between the axial HV electrode and the inner surface of the dielectric.

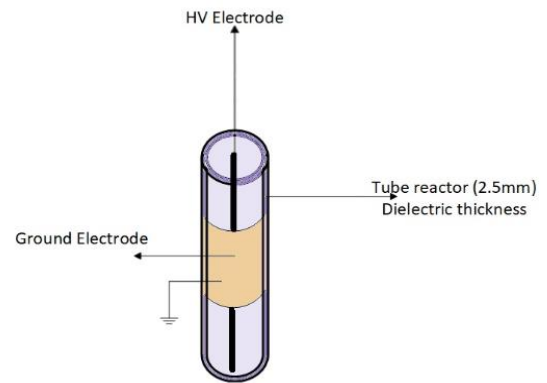


Figure 1 Schematic diagram of the reactor

Figure 1 presents the schematic diagram of the reactor and Figure 2 demonstrates the designed 3D geometry of the reactor in COMSOL.

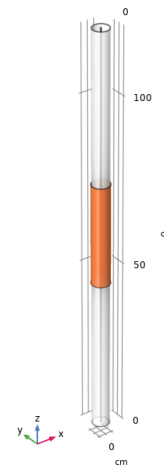


Figure 2 COMSOL model- Reactor 3D-geometry

The 3D model geometry features are as follows:

vertical axis (z) indicates the length of the tube which is 1.2 m; HV electrode is a stainless steel cylinder of 2.5 mm radius and 1.18 m length, the outer radius of the dielectric (quartz) tube is 25mm and it has a thickness of 2.5 mm, the ground electrode is made of copper and covers 30 cm of the length of the tube in the middle and at its outer circumference. The relative permittivity of nitrogen and quartz are 1 and 4.2, respectively.

By applying high voltage to the inner electrode, a strong electric field is generated in the gap between two electrodes. The electric field flux moves from HV electrode towards the ground electrode. Obviously, in case of applying AC voltage, the direction of electric field follows the alternating voltage.

In realistic application, the plasma is generated when the electric field is much high to promote the dielectric breakdown of the gas. In the presence of a strong electric field, free electrons gain enough energy to initiate the ionization reactions. Created electrons move toward the boundary surfaces in the opposite direction to the electric field. An equal number of ions (electrons and ions are generated in equal pairs) moves in the same direction of the electric field. Therefore, surface charge with opposite sign accumulates on both boundary surfaces.

3. Governing Equations

In this section, the governing equations of electrostatics physics that were used in the COMSOL simulation is briefly discussed.

The numerical study of the model and identifying equations involved, bring the fundamental interaction between electric field, and charged particles, also between charged particles and neutral gas molecules. The equations in this study are based on Gauss's law

$$\nabla \cdot E = \frac{\rho}{\epsilon_0}$$

where E is electric field, ρ is the total volume charge density and ϵ_0 is the permittivity of free space.

The electric displacement (D) is an important parameter and it involves free charge:

$$\nabla \cdot D = \rho$$

In case of linear materials, E is directly proportional to D which is presented as:

$$D = \epsilon E = \epsilon_0 \epsilon_r E$$

where ϵ_r is the relative permittivity of the gas.

For nonlinear materials, this relationship is presented as:

$$D = \epsilon_0 \epsilon_r E + D_r$$

D_r is the remnant displacement and it is the displacement in the absence of the electric field.

In order to find a distinctive solution, it is necessary to consider the boundary conditions as well. The boundary conditions would represent the interface between different media and follows the following equations:

$$n_2 \cdot (D_1 - D_2) = \rho_s$$

where n_2 is the outward normal from medium two, which in this case is dielectric.

Different medium behaves differently when it comes to electric charges. In dielectric materials, charges can displace within atoms or molecules, this displacement is far from migration of charges in conductors. By applying an external electric field to a dielectric material, the positive charges of its molecule are displaced along the field and negative charges are displaced in the opposite direction of the field.

4. Simulation Results and Discussion

This section presents the simulation results and a brief discussion about all different studied scenarios.

Case 1

Reactor design shown in Figure 2

In this study, the electric field distribution was investigated at different sections in the radial direction of the reactor when a 20kV dc voltage was applied to the HV electrode.

Figure 3 shows the surface electric potential in the scale of 0-20kV.

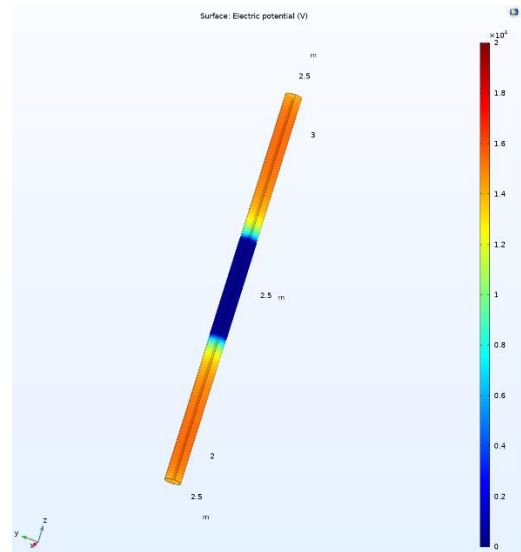


Figure 3 Surface electric potential

The potential decreases from 20 to 0 kV moving from the HV electrode surface toward the ground in the middle of the reactor, where the ground electrode is located. The rest of the tube surface shows that the voltage would not reach to zero and is in the range of 12 to 15 kV. That is due to the length of the ground electrode which only covers part of the reactor.

Electric field norm is one of the important parameters in modelling and simulation of the plasma. If the electric field norm exceeds the onset condition about mega volt per meter, the plasma occurs.

Figure 4 demonstrates the changes of electric field norm at different cross sections of the reactor. $z=0$ shows the middle of the tube (vertical length), $z=0.15$ shows the cross section at the edge of the ground electrode and $z=0.60$ shows the cross section at the top of the reactor. (for more details please check Appendix A). The x-axis in this graph shows the reactor radius from HV electrode centre (0) to the ground electrode surface at 0.026 m and y-axis presents the electric field norm magnitude. Electric field norm is decreasing exponentially by moving toward the inner surface of the tube. Then the value decreases suddenly at the boundary between the discharge gap and glass wall, then increase again in the corresponding to the outer surface of the glass due to the presence of the ground.

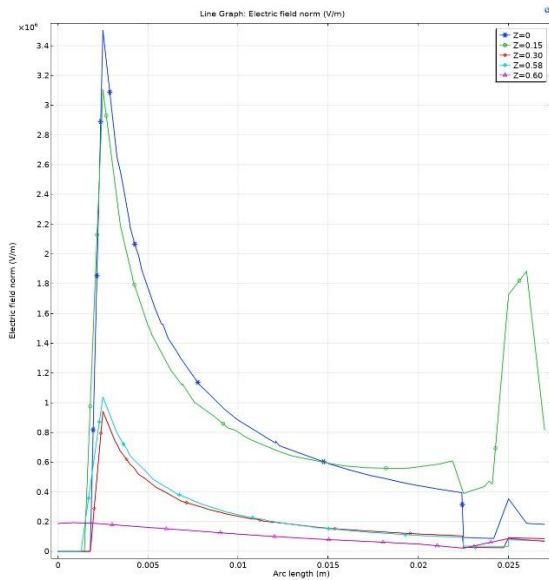


Figure 4. Electric field norm at different cross sections

Regardless of the cross-section plane, maximum value for the electric field norm happens at the gap near the HV electrode (at a radius of 2.5 mm around the HV electrode) and it decreases towards the surface of the dielectric tube ; although the magnitude is still in the range of 10^6 V/m, the changes are significant. The peak level of electric field is observed in the parts of the tube which has been covered by ground electrode. At edge of the ground electrode there is a sharp increase in the

electric field norm which is due to the electric field flux tend to create a close path.

In the parts of the tube above the ground electrode (between $z=0.3$ and $z=0.58$) the peak value for electric field norm is about 1MV/m and finally at the $z=0.6$ the lowest level of the electric field norm is observed.

Figure 5 shows the electric field at longitudinal side of the reactor, at different distances from HV electrode. In this graph, x-axis shows the length of the reactor which is 1.2 m and y-axis shows the electric field norm magnitude. The interval between 0.45 m and 0.75 m is the region in which ground electrode has covered outer surface of the reactor.

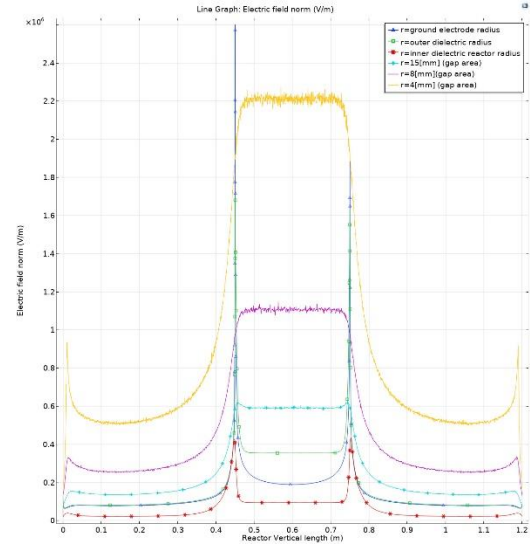


Figure 5. Electric field norm along vertical length of the reactor

As Figure 5 presents electric field increases as one approach the first edge of the ground electrode position and remains constant within the well-defined ground electrode region. As you pass the other edge of the ground electrode, the field values drop significantly as expected.

When the plasma is formed there will be radicals, ions, and electrons in the gas gap which in this model has not been considered; but to understand the behaviour of these species, the effect of the additional free space charges on the electric field norm was assessed by increasing the space charge density from 1.6×10^{-6} to $1.6 \times 10^{-2} C/m^3$. Hence, in addition to the applied field, the space charge field plays a part, in that at the inner surface of the dielectric more charge species will get accumulated and this results in increased amplitude of the electric field.

It was observed that a space charge density of $1.6 \times 10^{-2} C/m^3$, significantly changes the electric field norm level in the region of the tube which is not covered by ground electrode . As shown in figure 6, the peak value of electric field in the cross sections up to the ground electrode edge is similar to the results obtained with no

space charge (Figure 4) but from cross section at $z=0.15$ up to the top of the reactor at $z=0.58$, the electric field peak is much higher in comparison with Figure 4 and the peak values reaches a value of 10^7 V/m.

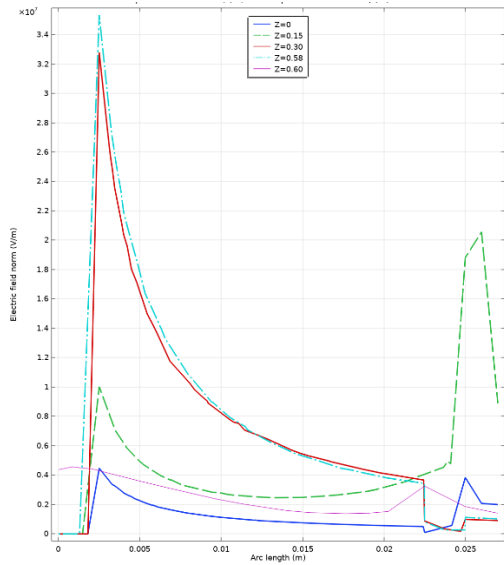


Figure 6 Electric field norm at different cross section when the space charge is $1.6 \times 10^{-2} \text{ C/m}^3$

Figure 7 shows the electric field at different radius along the tube length in the presence of $1.6 \times 10^{-2} \text{ C/m}^3$ space charge. Contrary to the figure 5, the field values increase outside the well-defined ground electrode region ($x < 0.45\text{m}$ & $x > 0.75\text{m}$) and decrease in the region where ground electrode covers the outer surface of the tube ($0.45 < x < 0.75\text{m}$). However, for all radii the electric field is much higher than the values at the same radius presented in Figure 4.

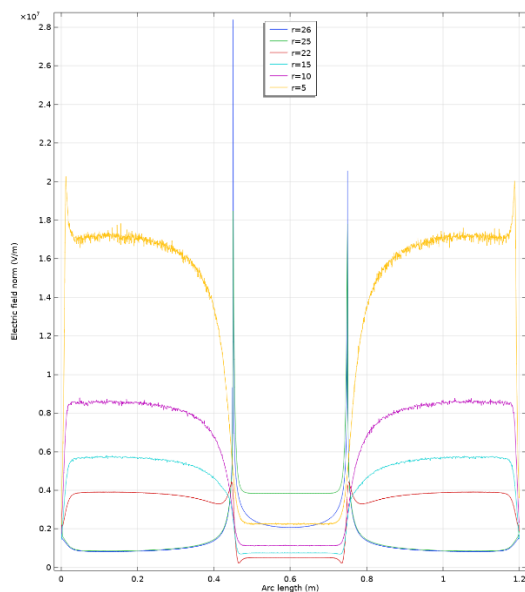


Figure 7 Electric field norm along the length of the reactor when the space charge is $1.6 \times 10^{-2} \text{ C/m}^3$

The above results suggest that the ground electrode configuration could have significant effect on the distribution of electric field and consequently non-thermal plasma characteristics. Therefore, the next section is to study two different locations and dimension for the ground electrode and compare the outcomes between these models and the main design.

Case2

1.2 m Ground electrode reactor

In the first attempt, the 30 cm length electrode was replaced by a 1.2 m length electrode to cover the full length of the tube. No other changes were applied to the geometry.

Figure 8 presents the electric field norm for different cross-sections when ground electrode is 1.2 m long.

As the graph shows, the electric field distribution behaves similar at different cross sections and would possibly provide same discharge along the gap. In contrast to Figure 4, the electric field reaches the peak value for all different cross sections. This may provide similar electric field intensity at the discharge gap for the full length of the tube which could be advantageous in initializing the plasma in full length of the tube. One of the disadvantages of this configuration is the elimination of visibility of the reactor which could not be used for visual investigation and measurement purposes of the plasma inside the tube.

Therefore, a third reactor design was considered based on multi ground electrode approach in which two ends of the outer surface of the dielectric tube was cover with 30 cm long ground electrodes (3D geometry image is available in the Appendix). All other features were kept unchanged.

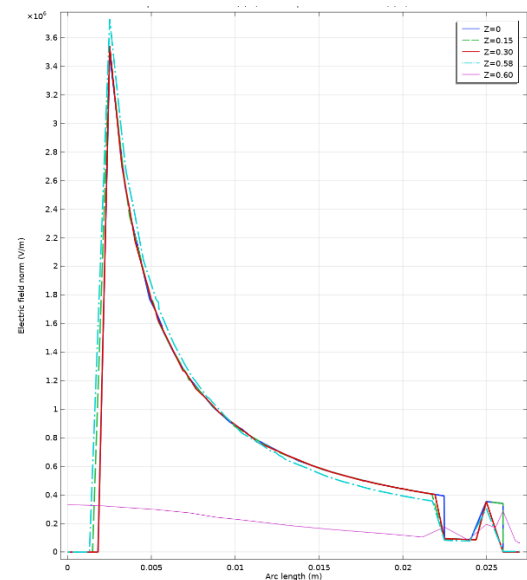


Figure 8. Electric field norm at different cross sections with 1.2 m length ground electrode

Figure 9 illustrate the simulation results at different cross sections; in this case, the cross sections at $z=0.3$ up to $z=0.6$ m, are the tube regions under the cover of ground electrode and the electric field norm reached its peak. At the edge of the ground electrode, there is a sharp increase ($z=0.3$ and $x=0.026$ m) which is much higher compared to what is shown in Figure 4 (cross section at $z=0.15$ at the edge of ground electrode).

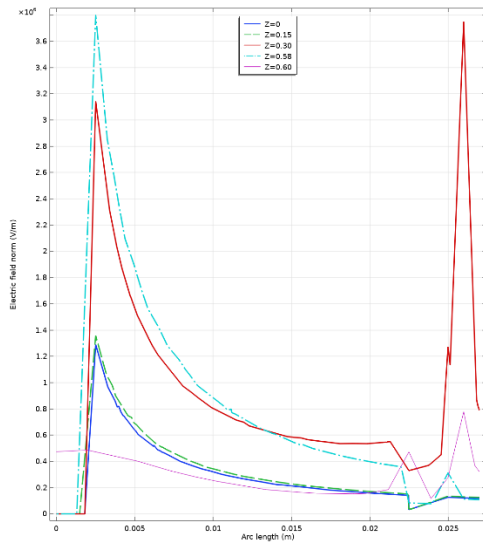


Figure 9 Electric field norm at different cross sections with 30 cm length ground electrodes at both ends of the reactor

Figure 10 demonstrate the changes of electric field at different radius along the full length of the tube. In comparison with Figure 5, the electric field shows higher level in the region of the well-grounded tube, but the maximum value is slightly lower as shown in Figure 10. On the other hand, the maximum level of electric field in the region of tube, which is not covered by ground electrode, is slightly higher.

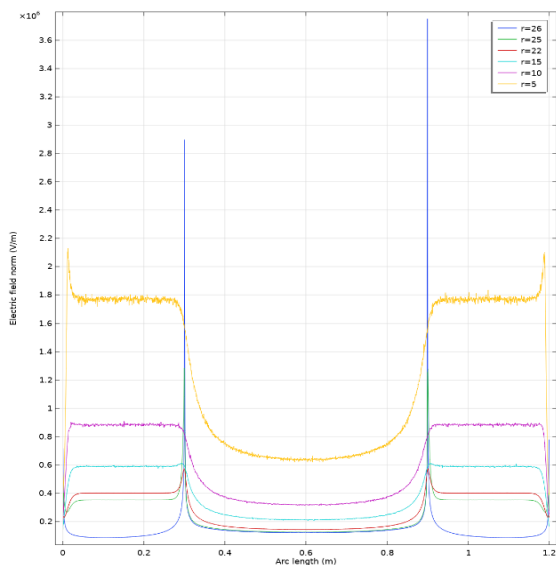


Figure 10 Electric field norm along vertical length of the reactor with ground electrode at both ends of the reactor

One of the advantages of this configuration is the possibility of visual monitoring and measurement of the plasma features through the interval between two ground electrodes.

Case 3

Parametric investigation of HV electrode radius

The next consideration is to assess the effect of the HV electrode radius on the electric field norm. Using parametric study, the HV electrode radius was changed from 1 mm to 16 mm in steps of 1.5 mm.

Electric field has invers relation with conductor cross section area, therefore as the HV electrode diameter decreases, the electric field should increase. But in case of the reactor, electric field is not only under the effect of the HV electrode diameter but the gas gap area (distance between two electrodes) which would affect the distribution of the electric field. As the gap between electrodes increases, the electric field decreases. Therefore, it is necessary to find a compromise between HV electrode diameter and the gap size between electrodes.

Figure 11 shows the electric field at $z=0$; the maximum level for electric field is recorded for 1 mm radius HV electrode. And it decreases as HV electrode radius increases to 8 mm; this is the bending point by which as HV electrode radius continuous to increase, the electric field is increasing too. The reason is that the gap between two electrodes decreases which in turn increase the electric field.

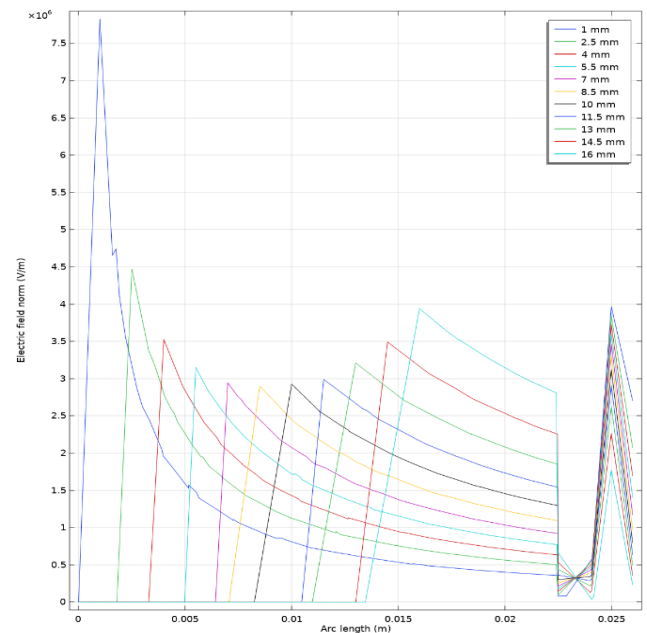


Figure 11 Electric field norm at $z=0$ for different HV electrode radius, 30 cm length ground electrode

Although 1mm radius provides the highest peak for electric field but the rate of change within the gap area is

very sharp while the 2.5 mm radius provides high enough electric field peak value. The rate of change within the gap area is not as steep as 1 mm radius electrode.

This study only considered the HV electrode diameter, but to find the most optimum design for the reactor, this study should be expanded further to include variable gap size and variable ground electrode dimension.

5. Conclusions

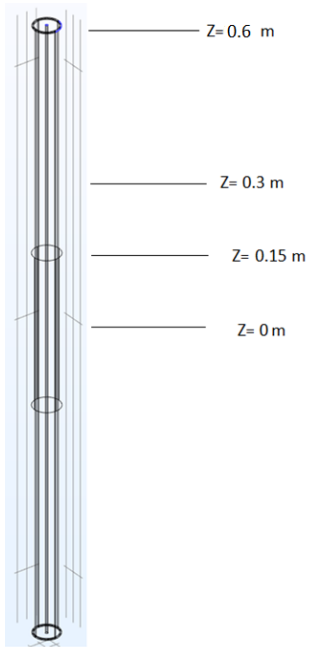
In this work, the electric field distribution of a non-thermal plasma reactor has been investigated using COMSOL using electrostatics module. In addition to the main design, the electric field distribution has been studied in the presence of the space charge density. In addition, the reactor with multi sections of ground electrode design has been studied. This work provides the primary understanding of the electric field distribution in an NTP using DBD approach and highlights the importance of the reactor design and effective parameters including HV dimension, ground electrode dimension and design, dielectric property, and thickness. This work can provide very useful information and initial design idea to find the optimum reactor design. However, further investigation needs to be undertaken using plasma module considering the chemistry of the plasma along with the electrostatic physics.

References

1. J. Meichsner, M. Schmidt, R. Schneider, H. Wagner, Nonthermal plasma chemistry and physics, CRC press, (2013)
2. W. Balachandran, N. Manivannan, R. Beleca, M. Abbod, D. Brenneb, N. Alozie, L. Ganippa, Nonthermal Plasma System for Marine Diesel Engine Emission Control, *IEEE transactions on industry applications*, Vol. 52, 2496-2505 (2016)
3. B.M. Penetrante, M. Hsiao, B. T. Merritt, G. E. Vogtlin, P. H. Wallman, comparison of Electrical Discharge Techniques for Nonthermal Plasma Processing of NO in N₂, *EEE TRANSACTIONS ON PLASMA SCIENCE*, VOL. 23, NO. 4, 679- 687, (1995)
4. R.B. Tyata, D.P. Subedi, C.S. Wong, Composition of Dielectric Barrier Discharge in Air, Nitrogen and Argon at Atmospheric Pressure, *Kathmandu University Journal of Science, Engineering and Technology*, **6**, 6-12 (2010)
5. F. Sohbatzadeh, H. Soltani, Time-dependent one-dimensional simulation of atmospheric dielectric barrier discharge in N₂/O₂/H₂O using COMSOL Multiphysics, *Journal of Theoretical and Applied Physics*, Vol12,53-63, (2018)

Appendix

Presentation of different cross sections on reactor.



Geometry of the reactor with two ground electrodes.

